Original Article

Effects of FGF2 Priming and Nrf2 Activation on the Antioxidant Activity of Several Human Dental Pulp Cell Clones Derived From Distinct Donors, and Therapeutic Effects of Transplantation on Rodents With Spinal Cord Injury

Hidefumi Fukumitsu[1] (iD)**, Hitomi Soumiya[1], Kaito Nakamura[1], Kosuke Nagashima[1], Makoto Yamada[1], Hiroyuki Kobayashi[1], Takahiro Miwa[1], Atsuki Tsunoda[1], Tomoko Takeda-Kawaguchi[2], Ken-ichi Tezuka[3], and Shoei Furukawa[1]**

Abstract

In recent years, the interest in cell transplantation therapy using human dental pulp cells (DPCs) has been increasing. However, significant differences exist in the individual cellular characteristics of human DPC clones and in their therapeutic efficacy in rodent models of spinal cord injury (SCI); moreover, the cellular properties associated with their therapeutic efficacy for SCI remain unclear. Here, using DPC clones from seven different donors, we found that most of the clones were highly resistant to H_2O_2 cytotoxicity if, after transplantation, they significantly improved the locomotor function of rats with complete SCI. Therefore, we examined the effects of the basic fibroblast growth factor 2 (FGF2) and bardoxolone methyl (RTA402), which is a nuclear factor erythroid 2-related factor 2 (Nrf2) chemical activator, on the total antioxidant capacity (TAC) and the resistance to H_2O_2 cytotoxicity. FGF2 treatment enhanced the resistance of a subset of clones to H_2O_2 cytotoxicity. Regardless of FGF2 priming, RTA402 markedly enhanced the resistance of many DPC clones to H_2O_2 cytotoxicity, concomitant with the upregulation of heme oxygenase-1 (HO-1) and NAD(P)H-quinone dehydrogenase 1 (NQO1). With the exception of a subset of clones, the TAC was not increased by either FGF2 priming or RTA402 treatment alone, whereas it was significantly upregulated by both treatments in each clone, or among all seven DPC clones together. Thus, the TAC and resistance to H_2O_2 cytotoxicity were, to some extent, independently regulated and were strongly enhanced by both FGF2 priming and RTA402 treatment. Moreover, even a DPC clone that originally exhibited no therapeutic effect on SCI improved the locomotor function of mice with SCI after transplantation under both treatment regimens. Thus, combined with FGF2, RTA402 may increase the number of transplanted DPCs that migrate into and secrete neurotrophic factors at the lesion epicenter, where reactive oxygen species are produced at a high level.

Keywords

human dental pulp cells, clonal difference, spinal cord injury, antioxidant factors, nuclear factor erythroid 2-related factor 2 (Nrf2) chemical activator (RTA402)

Introduction

The spinal cord is the nerve-conduction pathway that connects the brain to the peripheral nervous system; thus, spinal cord injury (SCI) results in deficits in the control of motor and sensory functions. SCI is caused by an external physical impact, such as that occurring in traffic accidents, falls, and sports-related injuries; alternatively, SCI results from an increase in the internal pressure of the spinal cord tissue caused by spinal canal stenosis, spinal tumors, and other conditions. Approximately 5,000–6,000 patients suffer from SCI annually in Japan, with 1 million (0.78–1.16 million) patients

[1] Laboratory of Molecular Biology, Department of Biofunctional Analysis, Gifu Pharmaceutical University, Gifu, Japan
[2] Department of Oral and Maxillofacial Surgery, Gifu University Graduate School of Medicine, Gifu, Japan
[3] Department of Stem Cell and Regenerative Medicine, Gifu University Graduate School of Medicine, Gifu, Japan

Corresponding Author:
Hidefumi Fukumitsu, PhD, Laboratory of Molecular Biology, Department of Biofunctional Analysis, Gifu Pharmaceutical University, 1-25-4 Daigakunishi, Gifu 501-1196, Japan.
Email: hfukumi@gifu-pu.ac.jp

reported worldwide[1–3]. In adult mammals, spontaneous axonal regeneration of the central nervous system, including the spinal cord, scarcely occurs; moreover, in the strictest sense, no effective and systematic treatment has been established for patients with SCI. Currently, surgical procedures to re-stabilize and decompress the spinal cord and augment blood pressure are being applied to reduce secondary damage in patients with acute SCI[4].

Recently, clinical research reports on the transplantation of mesenchymal stem cells (MSCs), mainly bone marrow–derived mesenchymal stem cells (BMSCs), have been rapidly accumulating, and stem cell therapy is expected to become a new treatment for many conditions, including SCI[5–7]. Conversely, dental pulp cells (DPCs) are expected to replace BMSCs as cellular therapeutic agents for the injured nervous system. DPCs are adhesive cells derived from dental pulp tissue and include prominently multiple MSCs that can differentiate into various cell lineages[8,9]. In addition, DPCs can be prepared from deciduous and third molar (wisdom) teeth that are otherwise disposed of as medical waste[10]. This renders them more advantageous than BMSCs in terms of the abundance of the cellular resources. For example, the preparation of DPC clones from human leukocyte antigen haplotype homologous (HHH) donors has been discussed, as they appear less frequently and cause less immune rejection, banking, and use of allogeneic cells for transplantation therapy[11,12]. Furthermore, some studies have demonstrated that DPCs induce a more effective functional recovery in animal models with SCI or stroke compared with BMSCs after cell transplantation[13,14].

After the primary physical damage, the blood vessels around the lesion epicenter in the spinal cord are disrupted, and neutrophils and macrophages infiltrate the parenchyma. These phagocytes in innate immunity release reactive oxygen species (ROS), including hydroxyl radicals, superoxide radicals, and hydrogen peroxide (H_2O_2), for bactericidal purposes. ROS production worsens the environment of the injured spinal cord within 3 h immediately after the primary damage, which will continue for 4 h[15]; i.e., the secondary injury processes that occur after ROS production are considered the main cause of pathological deterioration progression[16,17]. In contrast, studies using animal models suggest that BMSC transplantation is more effective for functional recovery when transplantation is performed during the acute or subacute phase (1–2 weeks after the injury) vs transplantation during the chronic phase (4 weeks after injury)[18,19]. Both the neuroprotective and anti-inflammatory effects of BMSCs and DPCs may explain the significant functional recovery observed after transplantation in acute SCI[20–22]. In fact, BMSCs and DPCs produce and secrete various anti-inflammatory and immunomodulatory cytokines and neurotrophic factors that promote neuroprotection and axonal regeneration[21,22]. Therefore, transplanted DPCs need to migrate to the lesion epicenter and produce such secretion factors, thus overcoming the increased ROS production and the deteriorating environment in the acute/subacute phase of the injury.

In a previous study, we reported that the basic fibroblast growth factor 2 (FGF2) enhanced the resistance of a DPC clone to ROS (H_2O_2) and facilitated the functional recovery of rats with SCI after its transplantation[23]. However, the therapeutic effect of DPCs in rats with SCI may vary significantly among different clones[24]. Therefore, in this study, we used several DPC clones from individual donors to examine the cellular properties (cell proliferation, migratory ability, resistance to H_2O_2-induced cytotoxicity, and locomotor-function recovery of SCI rats after transplantation) of each clone and found that many of the clones that exhibited a high treatment efficacy in rats with SCI displayed a high antioxidant capacity. In addition, we examined the expression of proteins related to cellular properties, such as antioxidant factors and major regulators of cytoskeletal rearrangement. Conversely, studies that investigated the reactivity of DPCs to residual monomers from dental composites and phytochemicals have shown that the activation of the nuclear factor erythroid 2-related factor 2 (Nrf2), which is a master transcription factor for antioxidant factors, enhances the antioxidant capacity of DPCs[25–28]. Therefore, we also examined the combined effect of an Nrf2 activator (bardoxolone methyl [CDDO-Me or RTA402]), which is a potentially useful therapeutic agent for cancer and inflammatory dysfunctions[29,30], and FGF2 on the antioxidant activities and cytoprotective effect of DPCs against oxidative stress, as well as their impact on the recovery of locomotor function in mice with SCI after DPC transplantation.

Materials and Methods

Ethics

This study was conducted ethically in accordance with the Declaration of Helsinki of the World Medical Association. All experiments using human DPCs were approved by the Ethics Committees of Gifu Pharmaceutical University and Gifu University and were performed according to the Ethical Guidelines for Medical and Health Research Involving Human Subjects in Japan and the Ethical Guidelines for Human Genome/Gene Analysis Research in Japan (Gifu Pharmaceutical University; approval numbers and date: 23-1, October 25, 2011; 28-17, January 11, 2017; 29-44, November 27, 2017; 30-33, November 14, 2018; 1-1, April 26, 2019; 2-16, November 6, 2020; and 3-25, September 16, 2021; Gifu University, approval numbers and date: 19-144, September 6, 2008; 22-280, April 26, 2011; 24-375, September 7, 2013; 26-116; July 9, 2014; 26-422; March 16, 2015; 28-335, December 21, 2016; 29-323, November 7, 2017; and 5-10, August 22, 2023). All participants provided written informed consent before enrollment in the study.

Isolation and Culture of Human DPCs

Dental pulp was collected from the third molars of patients at Gifu University Hospital, each of whom provided informed consent. DPCs were prepared as reported previously[31,32]. Subsequently, the DPCs were expanded in MSCGM medium (PT-3001, Lonza Group Ltd, Basel, Switzerland). The medium was changed every 3 days, and the cells were sub-cultured using TrypLE Express (12605-010, Thermo Fisher Scientific Inc, Waltham, MA, USA). DPC clones were sequentially named DPXXX in the order in which they were prepared and stocked (the stage of the dental pulp and the sex and age of the donor are provided in Supplemental Table 1).

After 10 passages, the DPCs were subcultured in 10% fetal bovine serum (FBS; HyClone, Logan, UT, USA) containing alpha MEM (M8042, Sigma-Aldrich, St Louis, MO, USA) (10% FBS-αMEM), with or without 10 ng/ml FGF2 (233-FB, R&D Systems Inc, Minneapolis, MN, USA) (DPXXXS and DPXXXF, respectively). All DPCs were cultured in their respective media and used in experiments after three to five passages. The DPCs were passaged every 3 days (at 1.0×10^6 cells/10-cm dish). For DPC-F, FGF2 (10 ng/ml) was supplemented daily to the culture medium. The DPCs were treated for about 2 weeks.

Animals

All animal experiments were approved by the Animal Care and Research Committee of Gifu Pharmaceutical University (approval numbers and date: 2014-289, January 15, 2015; 2015-172, October 13, 2015; 2019-010, April 12, 2019; 2019-036, April 22, 2019; 2020-056, June 24, 2020; 2021-056, August 23, 2021; and 2023-060, November 30, 2023) and were performed in compliance with the Guidelines for the Management and Welfare of Experimental Animals of the US National Institutes of Health. In addition to minimizing animal suffering and the number of animals used, all animal housing and experiments were conducted in strict accordance with the institutional Guidelines for the Care and Use of Laboratory Animals. Moreover, all animal experiments were performed and reported in accordance with the ARRIVE Guidelines 2.0 [https://arriveguidelines.org/resources/author-checklists (accessed on December 27, 2022)]. The reproducibility of all the data was confirmed by an independent replicate experiment.

To generate the rat SCI model, 57 female rats were used (27 for Fig. 1; 38 for the replication experiments). The rats were randomly divided into three groups, as follows: transplantation groups of either one of the two DPC clones (DP74F or DP296F) and the corresponding control ($n = 9$, and $n = 12$–13 for each group, respectively). To generate the mouse SCI model, 75 female mice were used (37 for Fig. 7; 38 for the replication experiments). The mice were randomly divided into three groups, as follows: DP296F transplantation group, RTA402-treated DP296F transplantation group,

and the corresponding control ($n = 12$–13, and $n = 11$–14 for each group, respectively). If an animal exhibited symptoms, such as rapid weight loss, humane endpoints were applied, and the affected animal was sacrificed by exsanguination from the abdominal aorta under isoflurane anesthesia. In addition, animals subjected to myelotomy died because of urinary tract dysfunction, including infection, hematuria, and dysuria (in total, 9 out of the 27 rats for Fig. 1 [11 out of 38 for the replication] and 11 out of the 37 mice for Fig. 7 [10 out of 38 for the replication] were excluded from the analyses).

Animal Surgery for Complete Transection of the Rat Spinal Cord and DPC Transplantation

Rat models of SCI with complete cord transection were generated as described previously[23]. Briefly, 7-week-old female Wistar rats (weight, 120–130 g at the beginning of the experiment) were anesthetized using a combination of three anesthetics, i.e., medetomidine hydrochloride, midazolam, and butorphanol tartrate. After laminectomy at the level of the 10th thoracic vertebra, the spinal cord was completely transected using microsurgical scissors. After the arrest of hemorrhage, the distal stump was carefully lifted to confirm complete transection, and it was ensured that the distal and proximal stumps were in contact when the former stump was returned to its original position. Immediately after surgery, DPCs [1×10^6 cells in 10 μl of phosphate-buffered saline (PBS) per rat] were transplanted into the gap between the rostral and caudal spinal cord stumps. After cell transplantation and suturing of the muscles and skin, the animals were unanesthetized by subcutaneous injection of atipamezole at 1 mg/kg and placed in standard cages, allowed free access to food and water, and maintained at 23°C ± 2°C with a 12-h light/dark cycle. Manual bladder evacuation was performed twice a day until recovery of bladder function was observed. For immunosuppression, the rats received daily intraperitoneal (i.p.) injections of cyclosporine A (10 mg/kg; C-6000, LC Laboratories, Woburn, MA, USA). All rat surgeries were performed by one operator (K.N.), to avoid potential confounding.

DPCs were subcultured in 10% FBS-αMEM containing 10 ng/ml FGF2 for 2 weeks. The DPCs were dissociated using TrypLE Express (Thermo Fisher Scientific Inc), and then washed with PBS three times before cell transplantation.

Animal Surgery for Compression Injury of the Mouse Spinal Cord and DPC Transplantation

SCI model mice with a spinal cord compression injury were generated as described previously[33], with slight modifications. Briefly, 7-week-old female ddY mice (weight, 28–30 g at the beginning of the experiment) were anesthetized using a combination of the three anesthetics mentioned above.
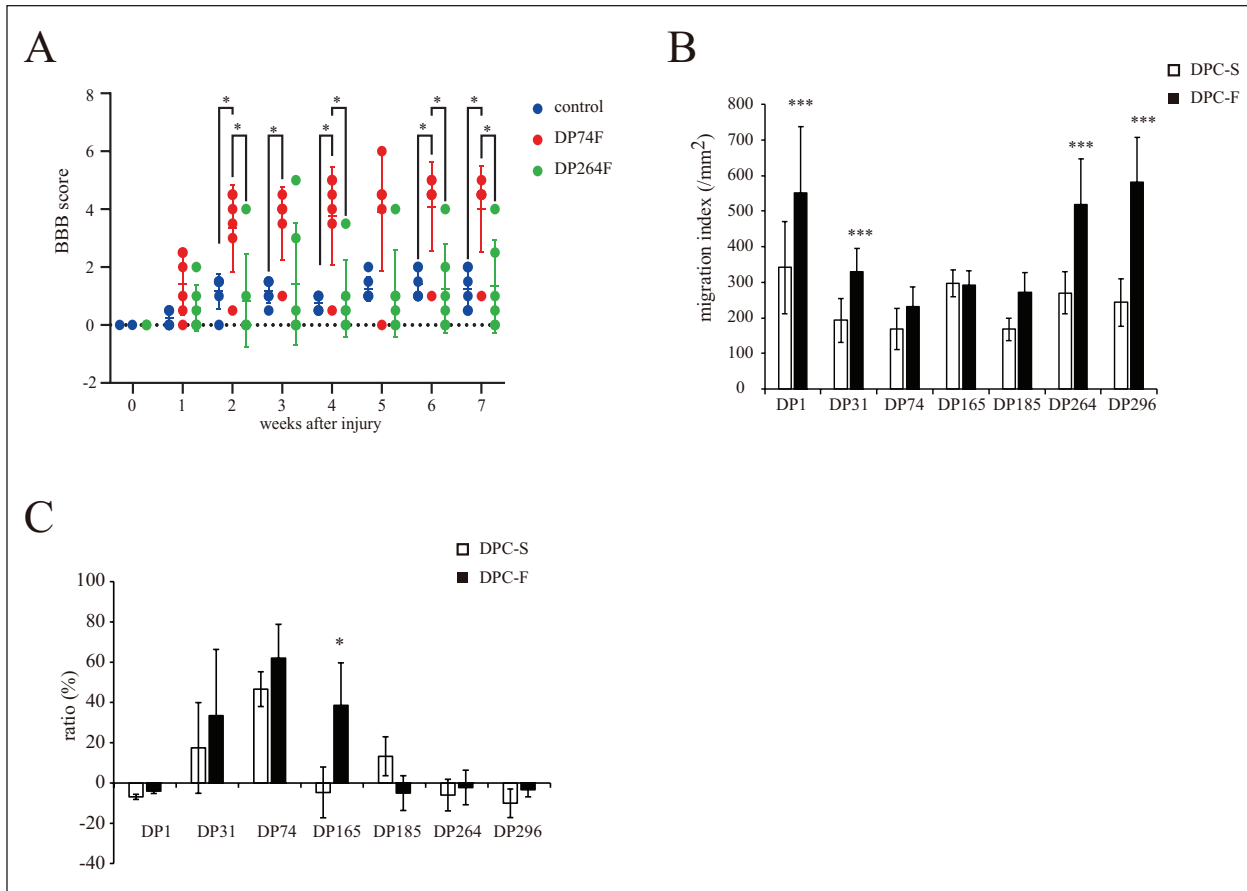
Figure 1. Effect of basic fibroblast growth factor (FGF2) priming on the properties of the seven individual donor-derived dental pulp cell (DPC) clones. (A) Effect of FGF2-primed DPC clone (DP74F or DP264F) transplantation on the locomotor function of rats with a completely transected spinal cord at the injury site. The locomotor function of the hind limbs was evaluated weekly for 7 weeks after injury. The values are expressed as individual scores with mean lines. Significant differences from the control group (rat with spinal cord injury with PBS injection) were determined using two-way repeated-measures ANOVA with post-hoc Tukey's multiple comparison test. $*P < 0.05$; $n = 6$ for each group. (B) Effect of FGF2 priming on the cell migration indices of the individual donor-derived DPC clones (DPC-S and DPC-F; DPC clones primed without and with FGF2, respectively). The values are expressed as the mean $\pm$ standard deviation (SD). Significant differences from the FGF2 non-treated groups were determined using two-way ANOVA with post-hoc Tukey's multiple comparison test. $***P < 0.0001$; $n = 12$ for each group. (C) Effect of FGF2 priming on the cell viability of 0.3 mM H_2O_2-treated individual donor-derived DPC clones. The values are expressed as the mean $\pm$ SD Significant differences from the FGF2 non-treated groups were determined using the two-way ANOVA with post-hoc Tukey's multiple comparison test. $*P < 0.05$; $N = 4$ ($n = 6$) for each group.

After laminectomy at the level of the 12th thoracic vertebra, an extradural spinal cord compression was performed using plastic microvascular clips with a closing power of 60 g/mm^2 for 15 s (Biover disposable vessel clip, DCM-1, DIADEM Industrial, Ibaragi, Japan). Subsequently, after the muscles and skin were sutured, the animals were injected intravenously (i.v.) with DP296F (1×10^6 cells in 0.3 ml of PBS per mouse), unanesthetized by subcutaneous injection of atipamezole at 1 mg/kg, and placed in standard cages. Manual bladder evacuation was performed twice a day until recovery of bladder function was observed. For immunosuppression, the mice received daily i.p. injections of cyclosporine A (10 mg/kg). All mouse surgeries were performed by one operator (H.K.), to avoid potential confounding.

For treatment with RTA402 (MedChemExpress, Monmouth Junction, NJ, USA), DP296 was subcultured in 10% FBS-αMEM containing 10 ng/ml FGF2 for 2 weeks, and the cells were treated with or without 150 nM RTA402 (final concentration) for 18 h. The DPCs were dissociated using TrypLE Express (Thermo Fisher Scientific Inc), and then washed with PBS three times before cell transplantation.

Assessment of Locomotor Function

The locomotor functions of the hindlimbs were assessed using the Basso, Beattie, Bresnahan Locomotor Rating Scale (BBB) (for rats) or the Basso Mouse Scale (BMS) (for mice) locomotor scale in the open field, as described previously[34–36].

The evaluation was performed 1 day after the administration of the injury, and it was subsequently performed once weekly by two observers (for rats, T.M. and H.S.; for mice, K.N. and A.T.) who were blinded to the experimental treatment, then continued for 7 (rats) or 5 (mice) weeks after injury.

Comparison of Cell Proliferation Rates

The cell proliferation rates were compared based on the doubling time. DPC clones were plated in parallel at 2.0×10^5 cells in 6-cm dishes. After 24, 72, and 144 h, the cells were washed with $1\times$ PBS, detached using TrypLE Express (Thermo Fisher Scientific Inc), and manually counted using a hemacytometer. The cells were passaged at 2.0×10^5 cells in a 6-cm dish every 3 days. The increase in cell count compared with the initial cell count was used to calculate the doubling time by assuming an exponential growth model. Nonlinear regression was performed using GraphPad Prism 9 version 9.5.1 for Windows (GraphPad Software Inc, San Diego, CA, USA), to fit the exponential phase to an exponential growth function. The doubling time was calculated by dividing ln (2) by the constant rate (k) obtained through nonlinear regression. The experiments were performed using seven to eight biological replicates.

Migration Assay

The migration of DPCs was evaluated using the *in vitro* scratch wound healing assay. DPCs were plated into type IP collagen (Cellmatrix Type lP; 638-0063, Nitta Gelatin Inc, Osaka, Japan)-coated 24-well plates at 6.0×10^4 cells/well and cultured with the respective growth medium for 24 h, to reach 100% confluence in the well. Then, a scratch (a cell-free zone) was made using a sterile 1,000-μl pipette tip, the cell debris was removed with serum-free α-MEM, and micrographs were acquired using an inverted microscope immediately afterward. Subsequently, at 24 h after culture, micrographs were collected again to observe cells migrating into the scratch. The migration index of each DPC clone was defined as the number of cells that migrated into the scratch over a period of 24 h (second micrograph) divided by the area of the scratch (first micrograph) (number/μm^2).

MTT Assay

Cell viabilities were compared based on the absorbance measured in the MTT assay. DPCs were plated at 4.0×10^3 cells/100 μl/well in 96-well plates. Twenty-four hours later, 100 μl of the respective medium was added per well (for DPC-S, 10% FBS-αMEM; for DPC-F, 10% FBS-αMEM with 10 ng/ml FGF2), and 100 μl of the medium was replaced with fresh medium containing various concentrations of H_2O_2. Twenty-four hours later, 10 μl of the 3-[4,5-dimethyl-2-thiazolyl]-2,5-diphenyl tetrazolium bromide (MTT, Sigma-Aldrich) solution (10 mg/ml in PBS) was added per well, and the DPCs were incubated for 4 h. After the dissolution of the crystals in HCl/isopropanol, the absorbance was measured at 570 nm using a microplate reader (Multiskan FC, 51119000 Thermo Fisher Scientific Inc). The average absorbance of the DPC-S treated with 0 mM H_2O_2 was regarded as 100%, and the percentage of the cell viability per well was expressed. Each experiment was performed using 6-well/96-well plates ($n = 6$) and was repeated four times ($N = 3$ or 4).

For RTA402 (MedChemExpress) treatment, 24 h after DPCs were seeded, 100 μl of the respective medium containing RTA402 (the final concentration of RTA is indicated in each figure legend) was added per well. Eighteen hours later, DPCs were treated with various concentrations of H_2O_2, and the MTT assay was performed at 24 h as described above.

Total Antioxidant Capacity Assay

DPC clones were plated in parallel at 3.0×10^5 cells in 6-cm dishes. At 24 h, the cells were cultured and treated with 150 nM RTA402 (final concentration) in their respective media for 18 h. DPCs were detached using TrypLE Express (Thermo Fisher Scientific Inc), washed with $1\times$ PBS three times, and lysed with 300 μl of ice-cold $1\times$ PBS via sonication for 1 min. The total antioxidant capacity (TAC) of the cellular lysate was measured using a chemical colorimetric method with a commercial antioxidant assay kit (OxiSelect TAC Assay Kit, STA-360, Cell Biolabs, Inc, San Diego, CA, USA). This method relies on the ability of the antioxidants in the sample to reduce copper (II) to copper (I), such as uric acid. Each experiment was performed using four dishes ($n = 4$).

Western Blot Analysis

Western blotting was performed as described previously[37,38]. Briefly, DPCs were washed with $1\times$ Tris-buffered saline (TBS) [10 mM Tris-HCl buffer (pH 7.4) containing 0.15 M NaCl] and lysed with lysis buffer [20 mM Tris-HCl (pH 7.4) containing 150 mM NaCl, 2 mM ethylenediaminetetraacetic acid (EDTA), 1% NP-40, 10 μg/ml aprotinin, 10 μg/ml leupeptin, 50 mM NaF, 1 mM Na_3VO_4, 1 mM phenylmethylsulfonyl fluoride, 0.1% sodium dodecyl sulfate, and 1% Na deoxycholate]. Each sample, containing 1–10 μg of proteins (depending on the target protein to be detected; Supplemental Table 2), was electrophoresed through sodium dodecyl sulfate polyacrylamide gel electrophoresis on 10% or 14% gels. The proteins were transferred to a polyvinylidene difluoride membrane (Pall Life Sciences, Portsmouth, UK), which was then blocked with 5% skim milk (Morinaga Milk Product, Tokyo, Japan) in 20 mM Tris-HCl (pH 7.4) containing 0.5 M NaCl and 0.05% Tween-20 at room temperature for 1 h. Subsequently, the membranes were incubated with primary antibodies (diluted with the appropriate blocking solution for the primary antibody used; Supplemental Table 2) at 4°C

overnight, washed, and reacted with alkaline phosphatase–conjugated antimouse or antirabbit IgG antibodies (as secondary antibodies) at room temperature for 1 h (Promega, Madison, WI, USA). Finally, protein bands were developed using nitroblue tetrazolium and 5-bromo-4-chloro-3-indoryl phosphate p-toluidine salt. The bands on Western blots were assessed by densitometric analysis using Image J (NIH Image, Bethesda, MD, USA).

Tissue Preparation for Immunohistochemical Analysis

Tissue preparation and an immunobiological analysis were performed as described previously[23]. Briefly, 5 weeks after injury and BMS scoring, mice were sacrificed for histological processing. The mice were cardio-perfused with a 4% paraformaldehyde (PFA) solution under terminal anesthesia via i.p. injection of sodium pentobarbital. Eight-millimeter-long spinal cord tissues, ie, 4.0 mm rostral and caudal to the lesion epicenter, were dissected and postfixed in 4% PFA overnight at 4°C. The tissues were then soaked in cold PBS containing 20% sucrose overnight at 4°C, and subsequently frozen in embedding compound (Sakura Finetek, Tokyo, Japan). Sagittal serial 25-µm-thick sections were prepared using a cryostat (model CM 1850; Leica, Nussloch, Germany), attached to adhesive-coated slides (Matsunami Glass, Bellingham, WA, USA), and dried before being used in immunofluorescence studies.

The sections were fixed with 4% PFA solution for 10 min at room temperature, then permeabilized for 30 min at 37°C with 0.3% (v/v) Triton X-100 in 0.1 M Tris-HCl buffer (pH 7.4). After washing with PBS, the sections were blocked for 30 min at room temperature in PBS containing 2% Block Ace, and then reacted with a diluted primary antibody specific for GFAP [1:1,000, GFAP (2E1) sc-33673, Santa Cruz Biotechnology, Santa Cruz, CA, USA] or 5-HT (1:5,000, 20080, Immunostar Inc, Hudson, WI, USA) overnight at 4°C. After washing with PBS, the sections were incubated with a fluorescence-conjugated secondary antibody overnight at 4°C [Alexa 546-conjugated goat antimouse IgG (A-11008) and Alexa 488-conduagated goat antirabbit IgG (A-11003), 1:1,000; Invitrogen, Waltham, MA, USA]. The slides were washed with PBS and coverslipped with CC/Mount (Diagnostic BioSystems, Pleasanton, CA, USA). Finally, the slides were imaged using an immunofluorescence microscope (BZ-X800 All-in-One; Keyence, Osaka, Japan).

Statistical Analysis

The data are expressed as the mean ± standard deviation. All statistical analyses were performed using GraphPad Prism 9 version 9.5.1 for Windows (GraphPad Software Inc) according to the Prism 9 Statistics Guide (https://www.graphpad.com/guides/prism/latest/statistics/index.htm). All details of the statistical analyses are described in the figure legends. Briefly, Student's *t*-test was used for significance testing between two groups. For multiple comparison testing, Turkey's multiple comparison tests were performed after a one- or two-way analysis of variance (ANOVA). In all cases, statistical significance was determined using a 95% confidence interval; therefore, $P < 0.05$ was deemed significant.

Results

Effect of FGF2 Pre-treatment on the Properties of Seven Distinct Donor-Derived DPCs

The hindlimb locomotor function of rats with complete spinal cord transection was evaluated after DPC transplantation: two DPC clones (DP74 and DP264) were prepared from two human donors aged 13–16 years and were cultured with FGF2 for three passages. Compared with the control group, the rat SCI group transplanted with DP74F showed a remarkable recovery of locomotor function. In contrast, the rat SCI group transplanted with DP264F exhibited no recovery of motor function (Fig. 1A). Previously, a similar evaluation was performed using five distinct donor-derived DPC clones, with some clones yielding no recovery of hindlimb motor function in rats with SCI after FGF2 pre-treatment followed by transplantation (transplantation effect, DP1F, DP31F, and DP165F; no transplantation effect, DP185F and DP296F[24]).

To address the basic cell biological properties of DPCs related to the locomotor-function recovery from the SCI after cell transplantation, the doubling time of DPCs primed with FGF2 was first examined using the above-mentioned DPCs derived from seven distinct donors. The doubling times of DP74, DP165, and DP185, as calculated using ln (2)/k, were less than 2 days; in turn, those of DP1, DP31, DP264, and DP296 were over 2 days, when the DPCs were cultured under FGF2-free conditions (Table 1 and Supplemental Fig. 1). FGF2 priming significantly shortened or tended to shorten the doubling times of most DPC clones (DPC-S vs DPC-F in DP1, DP31, DP264, and DP296, $P = 0.0006$, $P = 0.0009$, $P < 0.0001$, $P < 0.0001$; and DP165 and DP185, $P = 0.1499$, $P = 0.1272$; respectively), with the exception of DP74 (longer, $P < 0.0001$). No relationship was observed between the doubling time and locomotor-function recovery among the seven FGF2-primed DPC clones (Table 1).

Next, we examined the migratory ability of cells using the wound healing assay. The cell motility migration index of DP1, DP165, DP264, and DP296 tended to be or was significantly greater than that of DP31, DP74, and DP185 cultured under FGF2-free conditions (DP1S vs DP31S, DP74S, and DP185S, $P < 0.001$, $P < 0.0001$, and $P < 0.0001$; DP165S vs DP31S, DP74S, and DP185S, $P = 0.09$, $P < 0.005$, and $P < 0.01$; DP264S vs DP31S, DP74S,

Table 1. Doubling Time of DPCs.

		DP1	DP31	DP74	DP165	DP185	DP264	DP296
Constant rate (k)	DPC-S	0.445	0.458	0.315	0.331	0.260	0.435	0.405
	DPC-F	0.548**	0.588**	0.144***	0.366	0.294	0.545***	0.541***
Doubling time (days)	DPC-S	1.45	1.51	2.20	2.10	2.67	1.60	1.71
	DPC-F	1.20	1.18	4.80	1.90	2.36	1.27	1.28

Effect of basic fibroblast growth factor (FGF2) priming on the growth of individual donor-derived clones (n = 7–8). The growth curves of individual dental pulp cell (DPC) clones were analyzed using nonlinear regression. The doubling times of DPC clones were calculated using ln (2)/k. **P < 0.001; ***P < 0.0001, the constant rate (k) was compared between DPC clones primed without and with the basic fibroblast growth factor (DPC-S and DPC-F, respectively), using the extra sum of the square F test.

and DP185S, P = 0.49, P = 0.06, and P = 0.07; DP296S vs DP31S, DP74S, and DP185S, P = 0.96, P = 0.46, and P = 0.42; respectively). FGF2 priming enhanced the cell motility migration index of several DPC clones (DPC-S vs DPC-F in DP1, DP31, DP264, and DP296, P < 0.001, P < 0.001, P < 0.001, and P < 0.001, respectively). The cell motility migration index of DP1, DP264, and DP296 was significantly greater than that of DP31, DP74, DP165, and DP185 cultured under FGF2-treated conditions (DP1F vs DP31F, DP74F, DP165F, and DP185F, P < 0.001, P < 0.001, P < 0.001, and P < 0.001; DP264F vs DP31F, DP74F, DP165F, and DP185F, P < 0.001, P < 0.001, P < 0.001, and P < 0.001; DP296F vs DP31F, DP74F, DP165F, and DP185F, P < 0.001, P < 0.001, P < 0.001, and P < 0.001; respectively). However, no relationship was observed between the migration index and the treatment efficacy (Fig. 1B).

To assess the antioxidative activities of DPCs, we examined the survival ratio at 24 h after treatment with 0.3 mM H_2O_2: treatment at this concentration of H_2O_2 induced a clear difference in the survival ratio of DPCs among the different clones; i.e., the averaged survival ratio of DP31, DP74, and DP185, but not that of DP1, DP165, DP264, and DP296, was over 10%, whereas that of DP74 was significantly higher than those of clones cultured under FGF2-free conditions (DP74S vs DP1S, DP31S, DP165S, DP185S, DP264S, and DP296S, P < 0.0001, P = 0.09, P < 0.0005, P < 0.0001, P < 0.0005, and P < 0.0005, respectively). FGF2 priming significantly enhanced DP165 (P < 0.05, Fig. 1C). Thus, with the exception of DP1, FGF2-primed DPC clones with therapeutic efficacy for SCI model rats (DP31F, DP74F, and DP165F) showed an increase of over 20% in the averaged survival ratio and a higher resistance to 0.3 mM H_2O_2 compared with DPC clones without therapeutic efficacy (DP185F, DP264F, and DP296F) (DP31F vs DP185F, DP264F, and DP296F, P < 0.01, P < 0.05 and P = 0.07; DP74F vs DP185F, DP264F, and DP296F, P < 0.001, P < 0.001, and P < 0.001; DP165 vs DP185F, DP264F, and DP296F, P < 0.01, P < 0.05, and P < 0.05; respectively). In addition, none of the parameters examined here was correlated with donor age and sex or the stage of tooth development (Supplemental Table 1).

Expression of Proteins Associated With the Antioxidant Activities of DPCs

The levels of expression of proteins associated with antioxidative activities were examined in DPCs by Western blotting. First, the effects of FGF2 priming on the expression of antioxidant factors [catalase, glutathione peroxidase (GPx)1/2, Nrf2, and heme oxygenase (HO)-1] after treatment of DP1 and DP31 with 0.3 mM H_2O_2 (Fig. 2 and Supplemental Fig. 2) were examined, because these two FGF2-primed DPC clones significantly differed regarding their resistance to H_2O_2-induced cytotoxicity (DP1S vs DP31S, P = 0.35; DP1F vs DP31F, P < 0.05; respectively, Fig. 1C). The expression levels of catalase and GPx1/2 were higher (~1.5-fold) after 0–3 h of exposure to H_2O_2 in DP31F vs DP31S, although these differences between the two groups were decreased after 6 h of exposure to H_2O_2 (up to 48 h, Fig. 2). Conversely, in DP1, FGF2 priming had little effect on the expression levels of catalase and GPx1/2, which tended to decrease at 48 h after H_2O_2 treatment (Fig. 2). No significant alterations were found in the expression levels of Nrf2 and HO-1 after FGF2 priming or H_2O_2 treatment (Supplemental Fig. 2).

Subsequently, the effects of FGF2 priming on the H_2O_2-induced catalase and GPx1/2 expression levels were examined in the seven DPC clones. Catalase expression in DP31 and GPx1/2 expression in DP74 and DP165 were significantly increased (Fig. 3A, B: 0 h and Fig. C, D: 3 h after 0.3 mM H_2O_2 treatment). The correlation between survival (after 24 h) and the expression of each antioxidant factor at 3 h after 0.3 mM H_2O_2 treatment was not statistically significant for catalase (R^2= 0.001, P = 0.77, Fig. 3D), whereas it was significant for GPx1/2 (R^2 = 0.67, P < 0.0001, Fig. 3E). Therefore, regardless of FGF2 priming, DPCs expressing a higher level of GPx1/2 at 3 h after 0.3 mM H_2O_2 treatment were more resistant to H_2O_2-induced cytotoxicity.

Effect of Nrf2 Activation on the Expression of Antioxidant Factors in DPCs

As described above, the expression of Nrf2, which plays an important role in oxidative stress defense, was
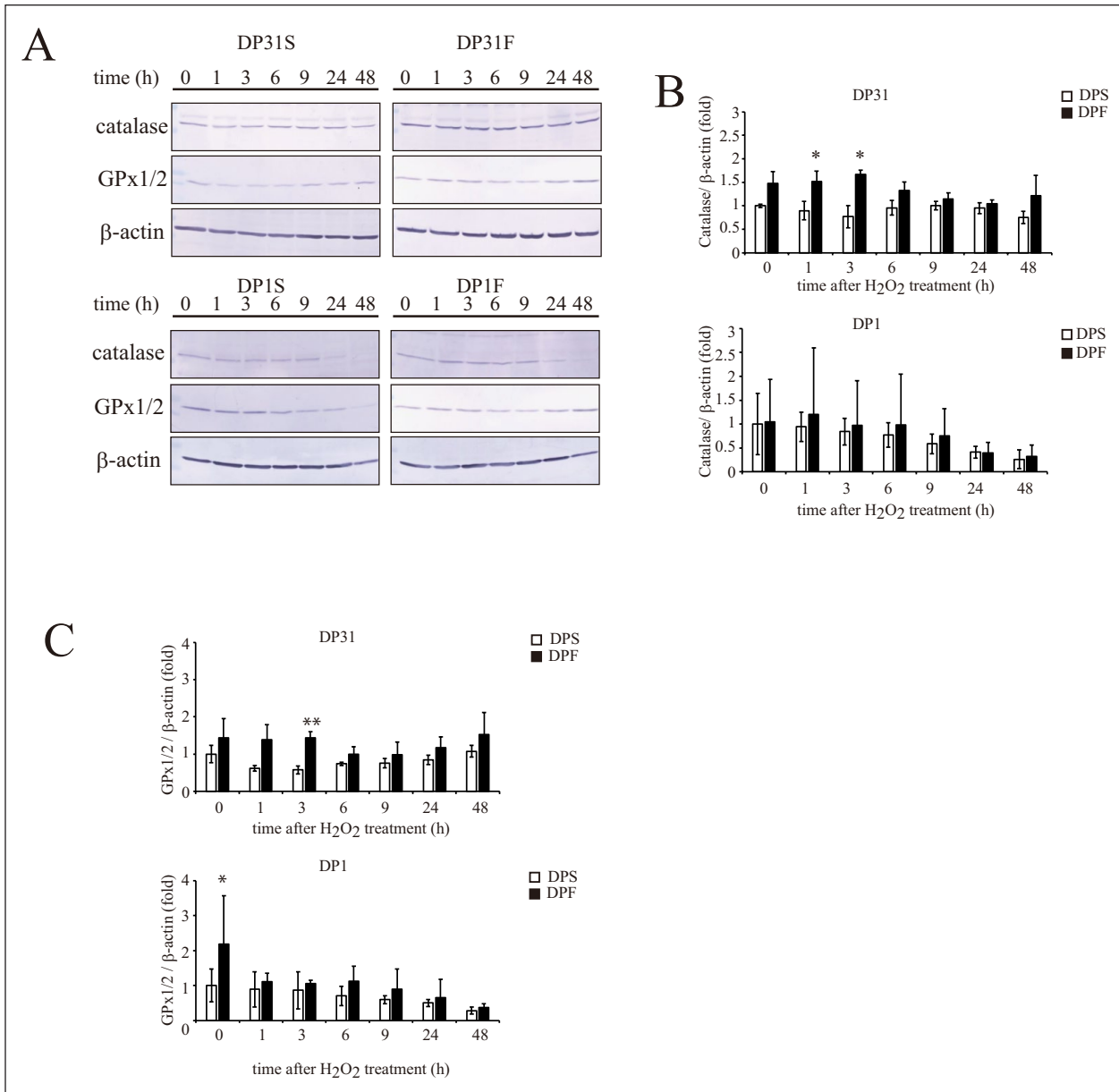
Figure 2. Effect of basic fibroblast growth factor (FGF2) priming on the time-dependent alterations in the expression levels of catalase and glutathione peroxidase 1/2 (GPx1/2) in DP1 and DP31 after treatment with 0.3 mM H_2O_2. A. DP1 and DP31 were treated with 0.3 mM H_2O_2. After the indicated periods, the expression levels of the catalase and GPx1/2 proteins were determined by Western blotting, together with the evaluation of β-actin as a loading control. The results obtained for catalase (B) or GPx1/2 (C) are reported as the mean ± standard deviation. Significant differences from the FGF2 non-treated groups were determined using two-way ANOVA with post-hoc Tukey's multiple comparison test. *$P < 0.05$; **$P < 0.01$, $n = 4$–5 for each group.

not significantly affected, and the expression of the protein product of its downstream gene, *HO-1*, even tended to decrease in the presence of FGF2 priming. Thus, the Nrf2 expression/activity and oxidative stress resistance of DPCs may not be sufficiently induced by FGF2 priming. Therefore, we investigated the possibility that an Nrf2 activator, RTA402, enhances the antioxidant capacity and resistance to H_2O_2-induced cytotoxicity of DPCs.

No significant increase in the TAC in DPC clones was induced by either FGF2 priming or RTA402 treatment alone, with the exception of DP31 (DPC-S vs DPC-F, $P < 0.001$), or DP165 and DP264 (DPC-S vs DPC-S+RTA402, $P < 0.05$ and $P < 0.01$, respectively). Because of a synergistic and/or additive effect, the TACs of DPCs were significantly increased by both FGF2 priming and RTA402 treatment compared with those detected in DPCs cultured under FGF2/
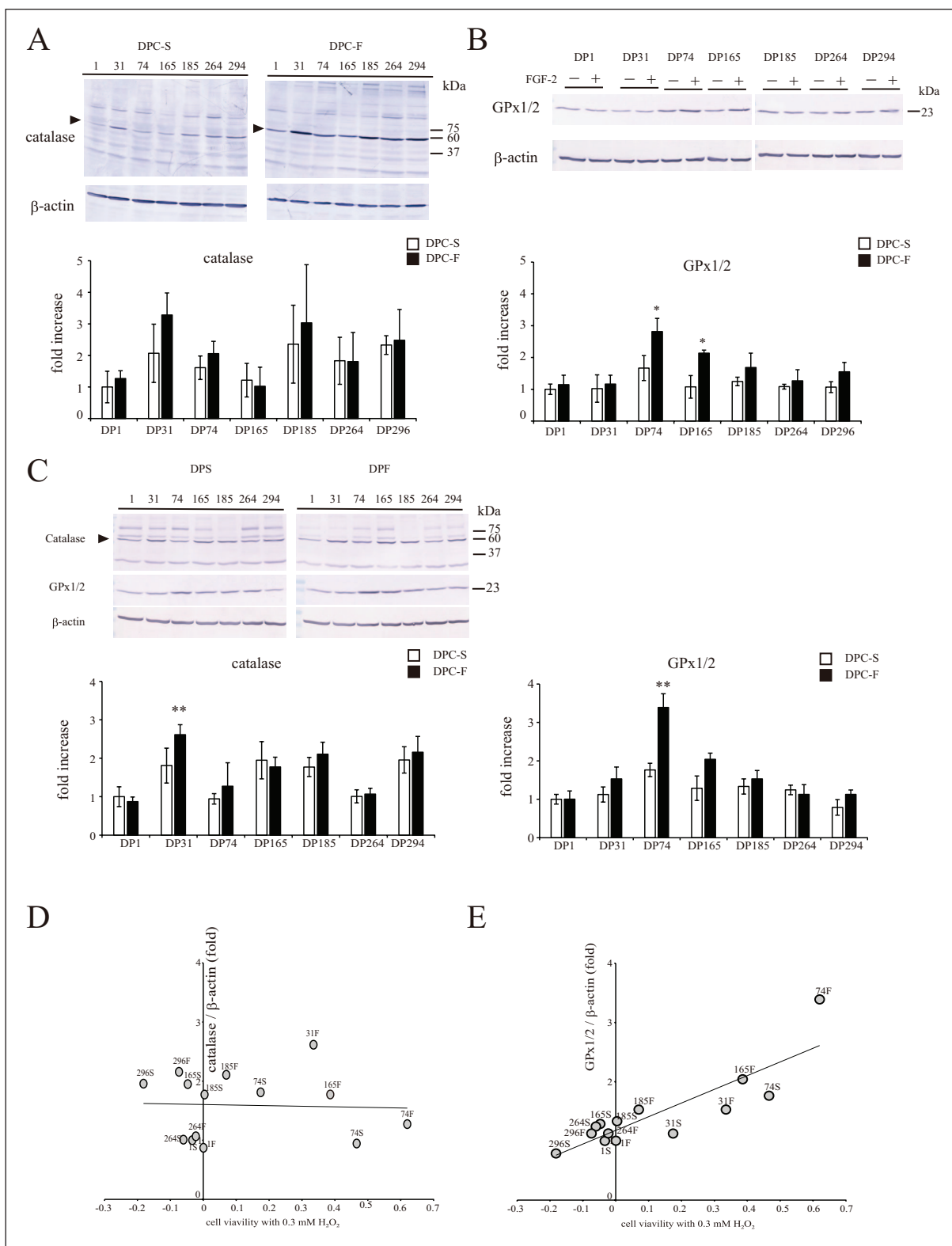
Figure 3. Effect of FGF2 priming on the expression levels of catalase and glutathione peroxidase 1/2 (GPx1/2) in individual donor-derived dental pulp cells (DPCs) after treatment with H_2O_2. Each DPC clone was treated with 0.3 mM H_2O_2. At 0 h (A, B) or 3 h (C) after the treatment, the expression levels of the catalase (A, C) and GPx1/2 (B, C) proteins were determined by Western blotting, together with the evaluation of β-actin as a loading control. The results obtained for catalase, or GPx1/2, are shown as the mean ± standard deviation. Significant differences from the FGF2 non-treated groups were determined using two-way ANOVA with post-hoc Tukey's multiple comparison test. *$P < 0.05$; **$P < 0.01$, $n = 4$–5 for each group. Correlation analyses of the expression levels of catalase (D) or GPx1/2 (E) with cell viabilities at 24 h after treatment with 0.3 mM H_2O_2.
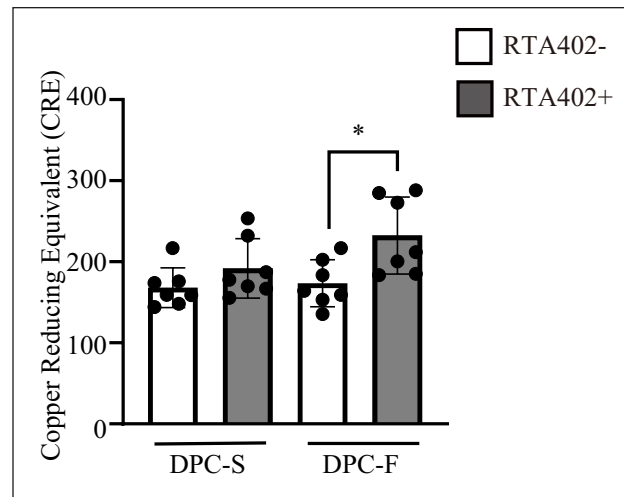
Figure 4. Effect of RTA402 and FGF2 on the total antioxidant activities of dental pulp cells (DPCs) [DPC-S and DPC-F; DPC clones primed without and with basic fibroblast growth factor (FGF2), respectively]. The values are expressed as the mean $\pm$ standard deviation (SD). Significant differences between groups were determined using two-way ANOVA with post-hoc Tukey's multiple comparison test. *$P < 0.05$, $n = 7$ average copper reducing equivalent of individual DPC clones for each group.

RTA402-free conditions, for each clone and among all clones together (DPC-S vs DPC-F+RTA402 and DPC-F vs DPC-F+RTA402, $P < 0.01$ and $P < 0.05$, respectively; Supplemental Table 3 and Fig. 4).

Conversely, the resistance to H_2O_2 cytotoxicity was significantly increased by RTA402 treatment in the DP1, DP31, and DP296 clones, regardless of FGF2 priming (Fig. 5). The cell viabilities of those RTA402-treated DPC clones after treatment with high concentrations of H_2O_2 (Fig. 5) were even more than comparable with those detected for DP31F, with significant therapeutic effects on rat SCI. Notably, the cytotoxicity of H_2O_2 depends on the lot, and the experiments depicted in Fig. 5 were carried out using different lots compared with those employed in the experiments reported in other figures. Thus, the cytoprotective effect against oxidative stress is thought to be regulated by RTA402 treatment or FGF2 priming at least partially independently of TAC (Figs. 1C and 5).

The expression of antioxidant factors, such as HO-1 (oxidative stress protection) and NAD(P)H-quinone dehydrogenase 1 (NQO1) (xenobiotic metabolizing enzyme), was concentration-dependently upregulated by RTA402 treatment in both DP31 and DP296 (Fig. 6), whereas the effective concentration of RTA402 and/or the effect of FGF2 priming on the expression of these factors differed according to clone. In contrast, the expression levels of catalase, the catalytic subunit of γ-glutamyl-cysteine ligase (γ-GCLc), and GPx1/2 were not affected by RTA402 treatment (Supplemental Fig. 4); these enzymes are known to detoxify H_2O_2, thus reducing oxidative stress.

Therefore, combined with FGF2 priming, RTA402 seemed to enhance the TAC and cytoprotective effect against oxidative stress in several DPC clones (Figs. 4 and 5 and

Supplemental Table 3), although the molecular mechanisms underlying these effects are likely to be slightly different in each clone, eg, protein expression of individual antioxidant factors (Figs. 3 and 6).

Effect of FGF2 Priming on the Expression of Neurotrophic Factors and p21-Activated Kinases in DPCs

For the functional repair of the injured spinal cord, it is important that the transplanted DPCs migrate to the lesion epicenter and produce and secrete neurotrophic factors. Therefore, we first examined the expression of p21-activated kinases (PAKs) 1 and 2 (Supplemental Fig. 3A–C) or tissue inhibitors of metalloproteinase 2 (TIMP2) (Supplemental Fig. 3A, D) in each DPC clone and analyzed the relationship between the expression levels of these factors and the migration index (Supplemental Fig. 3E, F). Both PAKs and TIMP2 are important factors for cell proliferation and migration and tissue invasion: PAKs regulate the rearrangement of the actin cytoskeleton[39,40] and TIMP2 inhibits matrix metalloproteinases from degrading extracellular matrix substrates[41]. The expression levels of these factors were similar among the DPC clones, and FGF2 priming significantly upregulated PAK1 and PAK2, but not TIMP2, across the seven clones (DPC-S vs DPC-F, $P < 0.005$, $P < 0.05$, and $P = 0.70$, respectively), although no significant differences were observed among individual donors (Supplemental Fig. 3A–D). Conversely, the migration index of DPC-S was correlated with the expression of TIMP2 (Supplemental Fig. 2E: TIMP2, $R^2 = 0.34$, $P < 0.0001$; PAK2, $R^2 = 0.005$, $P = 0.47$, respectively), whereas that of DPC-F was positively correlated with PAK2 (Supplemental Fig. 3F: TIMP2, $R^2 =$
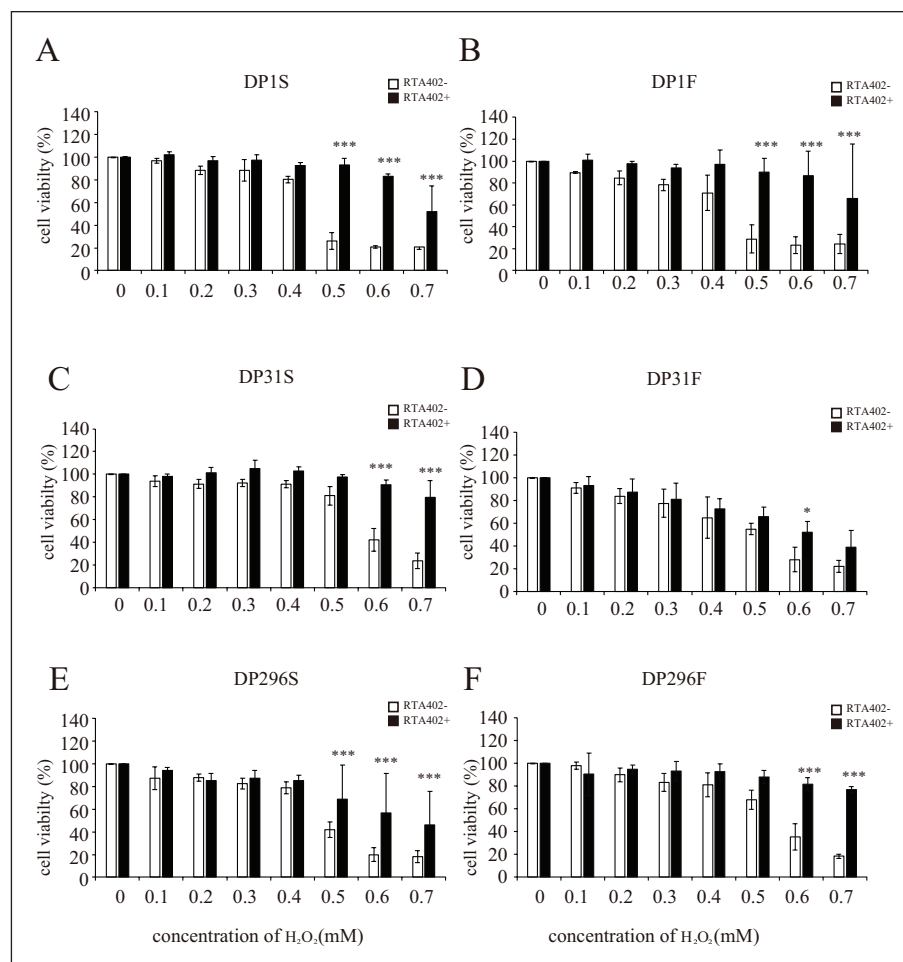
Figure 5. Effect of RTA402 on the resistance to H_2O_2-induced cell death in individual donor-derived dental pulp cells (DPCs) [DPC-S and DPC-F; DPC clones primed without and with basic fibroblast growth factor (FGF2), respectively]. After priming with/without FGF2 and treatment with/without 150 nM RTA402, each DPC clone (A, B: DP1; C, D: DP31; and E, F: DP296) was exposed to H_2O_2 at various concentrations (0, 0.1, 0.2, 0.3, 0.4, 0.5, 0.6, and 0.7 mM) for 24 h, followed by the MTT assay. The ratios of the absorbance values recorded for the DPCs exposed to H_2O_2 were calculated relative to the control (neither H_2O_2- nor RTA402-treated DPCs). The values are expressed as the mean ± standard deviation. Significant differences between the two groups were determined by two-way ANOVA with post-hoc Tukey's multiple comparison test. *$P < 0.05$; **$P < 0.01$; and ***$P < 0.001$ vs DPC without RTA402 treatment with H_2O_2 at the same concentration; $N = 3$ ($n = 6$) for each group.

0.07, $P < 0.001$; PAK2, $R^2 = 0.57$, $P < 0.0001$, respectively), suggesting that PAK2 is a key regulator of FGF2-induced DPC migration. The FGF2-induced upregulation of either PAK1 or PAK2 was not affected by RTA402 treatment in DP31 and DP296 (Supplemental Fig. 5).

Next, we examined the expression levels of the brain-derived neurotrophic factor (BDNF), glial cell line-derived neurotrohpic factor (GDNF), and hepatocyte grouwth factor (HGF) proteins, which are neurotrophic factors that promote neuroprotection and axonal regeneration in the injured spinal cord[42–44]. Using the average data of individual clones (total of seven clones), no significant alterations in the expression of the neurotrophic factors were observed after FGF2 priming and RTA402 treatment alone, or both; in turn, the expression of GDNF was slightly but significantly

increased by FGF2 priming (Supplemental Fig. 6). Thus, FGF2/RTA402 treatment may have enhanced, but it did not seem to attenuate the production of neurotrophic factors by DPCs.

The Activation of the Antioxidant Capabilities of DPCs Improves the Locomotor Function of SCI Model Mice After Their Transplantation

Finally, the therapeutic effects of DPCs pre-treated with FGF2/RTA402 on the SCI model were investigated. Considering the previous reports of the application of BMSCs using various delivery methods for the successful functional recovery of SCI model animals, in this study, we examined the effect of a single i.v. administration of DPCs
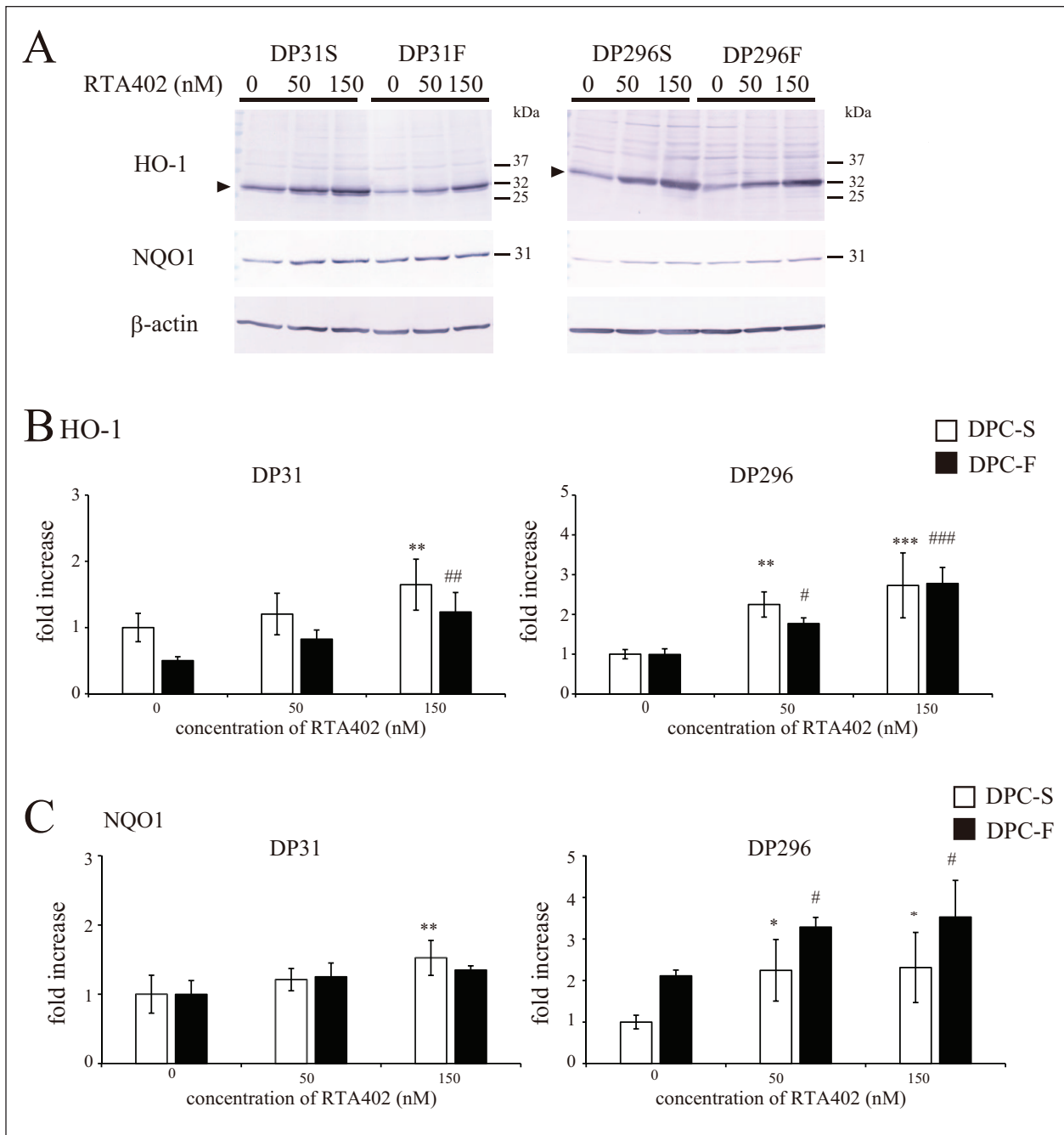
Figure 6. Effect of RTA402 on the expression levels of the heme oxygenase-1 (HO-1) and NAD(P)H-quinone dehydrogenase 1 (NQO1) proteins in DP31 and DP296 primed with basic fibroblast growth factor (FGF2). After priming with/without FGF2, each dental pulp cell (DPC) clone was treated with various concentrations of RTA402 (0, 50, and 150 nM) for 24 h. (A) The expression of the HO-1 and NQO1 proteins was determined by Western blotting, together with the evaluation of β-actin as a loading control. The results obtained for HO-1 (B) or NQO1 (C) are shown as the mean $\pm$ standard deviation. Significant differences between the two groups were determined by two-way ANOVA with post-hoc Tukey's multiple comparison test. *$P < 0.05$; **$P < 0.01$, and ***$P < 0.001$ vs DPC-S untreated with H_2O_2 and #$P < 0.05$; ##$P < 0.01$, and ###$P < 0.001$ vs DPC-F untreated with H_2O_2, $n = 4$ for each group.

on mice with spinal cord compression injury. After i.v. injection of DP296, SCI model mice exhibited a slight but significant recovery of locomotor functions in cases in which the cells were pre-treated with FGF2/RTA402, but not with FGF2 alone (Fig. 7A). Notably, the locomotor functions of

the SCI model mice were determined using the BMS score, because BMS is considered to be a sensitive, valid, and reliable method to measure locomotor functions in SCI model mice[35,36]. In addition, an immunohistochemical analysis revealed that the number of descending 5-HT[+]-nerve fibers,
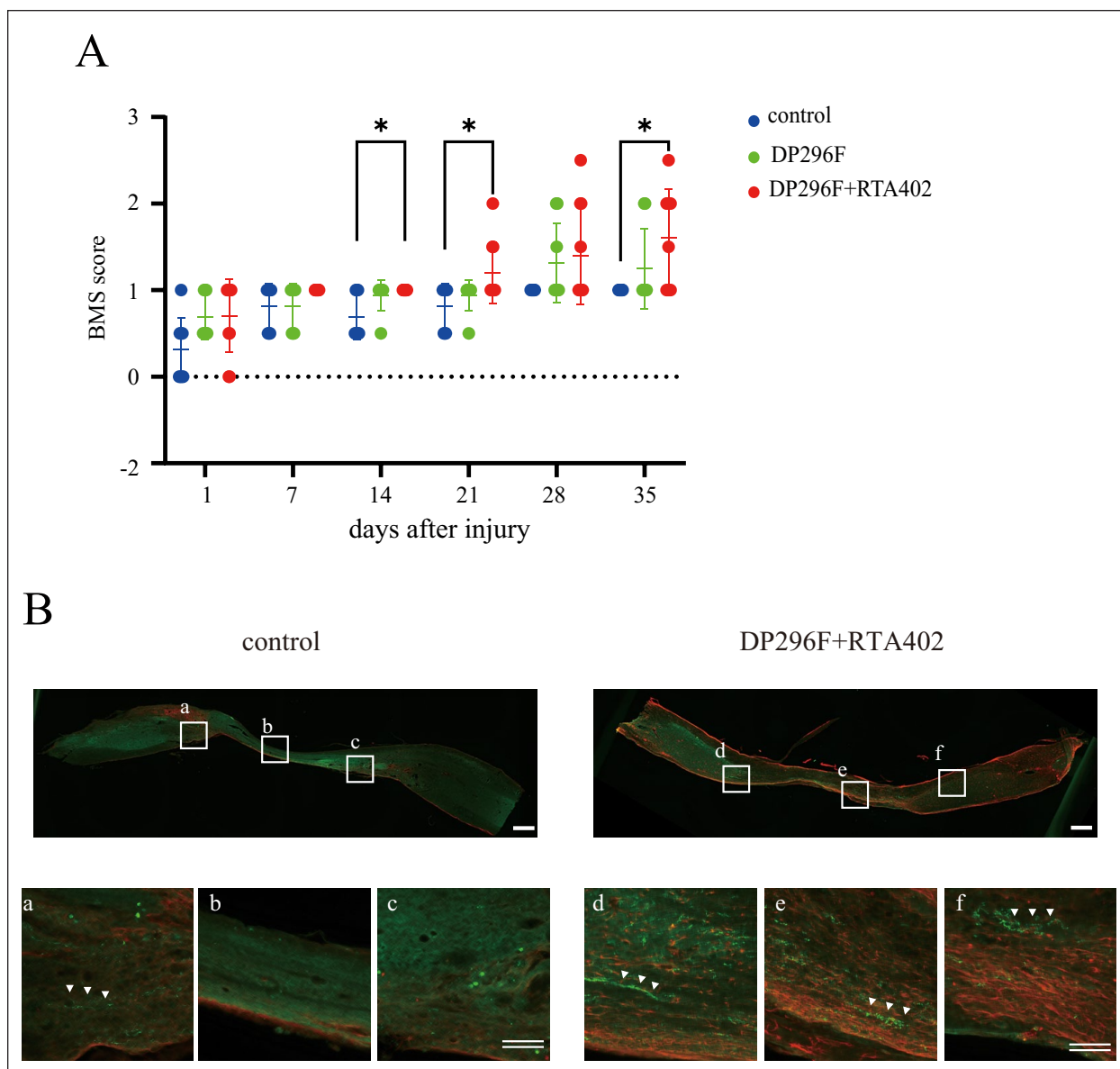
Figure 7. Effect of the i.v. transplantation of DP296F treated with/without RTA402 (DP296F+RTA402 or DP296F) on the locomotor function of mice with a compression spinal cord injury (SCI). (A) The locomotor function of the hind limbs was evaluated weekly for 5 weeks after injury. The values are expressed as individual scores with mean lines. Significant differences from the control group (SCI mice with PBS injection) were determined using two-way repeated-measures ANOVA with post-hoc Tukey's multiple comparison test. $n =$ 8–10 for each group. (B) At 5 weeks after cell transplantation, an immunohistochemical analysis was performed using the central sagittal section of the spinal cord tissues. The lower panels depict a higher magnification of the boxed regions in the upper panels. Note that a measurable number of 5-HT$^+$-nerve fibers were detected in the DP296F+RTA402 groups (three out of four), but not in the remaining groups (0 out of four) below the caudal edge of the injury sites. Single scale bar, 500 μm; double scale bars, 100 μm; respectively.

which is closely related to locomotor function, was greater in the lesion epicenter of the DP296F+RTA402 group compared with those of the control and DP296F groups at 5 weeks after transplantation (Fig. 7B).

Discussion

Previous studies have examined the basic properties of human DPCs in various culture conditions and used cells prepared from dental tissues from donors with distinct ages. Many DPCs exhibit a mitotic frequency of 40–60 generations or more, and donor age has been reported to affect the doubling time[45,46]. In contrast, the doubling time and migration capacity of DPCs are more strongly influenced by individual differences than that are by donor age[46,47]. In this study, we examined the TAC, the resistance to H$_2$O$_2$ toxicity and therapeutic efficacy for SCI, together with the doubling time and migration capacity of seven independent DPC

clones derived from donors with distinct ages and sexes. Because all parameters could not be categorized according to donor age (or the developmental stages of the dental pulp), they would be also attributed to the individual differences of the DPC clones. Furthermore, FGF2 priming significantly shortened the doubling time and enhanced the migration of many DPC clones and the resistance to H_2O_2-induced cell toxicity in certain DPC clones; however, no relationship was found among the FGF2-induced alterations in parameters (Fig. 1). Thus, it is suggested that FGF2 treatment can induce a variety of DPC properties associated with their therapeutic effect on the SCI model after transplantation; however, the affected parameters and degree of enhancement are also more strongly influenced by individual differences than they are by the age of the donor of the DPC clone.

Effects of FGF2 and Nrf2 Activators on the Expression of Antioxidant Factors and TAC in DPCs

Similar to the resistance to H_2O_2 cytotoxicity, the effect of FGF2 priming on the expression of antioxidant factors also differed among the DPC clones; catalase expression in DP31 (Fig. 3A, C) and GPx1/2 expression in DP74 and DP165 (Fig. 3B, C) were significantly increased, respectively. Among all seven clones taken together, higher expression levels of GPx1/2, which has H_2O_2-degrading activity[48], resulted in a greater survival activity of DPCs upon H_2O_2 treatment (Fig. 3E). However, focusing on two specific clones (DP74 and DP165), no relationship was observed between FGF2-induced GPx1/2 expression and the resistance to H_2O_2 cytotoxicity (Figs 1 and 3). In addition to the fact that FGF2 priming alone did not affect the TAC, these results indicated that the antioxidant capacities and resistance to H_2O_2 cytotoxicity in DPCs were at least partially independently regulated; these two parameters in individual DPC clones may be regulated by selecting distinct subsets of genes among various related enzyme groups.

Nrf2 is a transcription factor that regulates the expression of over 300 target genes with roles in antioxidant and electrophile detoxification[49,50]. Several chemicals that activate Nrf2 also suppress ROS-induced DPC death[26–28]. Therefore, Nrf2 activation was expected to be an effective means of comprehensively enhancing the antioxidant capacity of DPCs. In fact, RTA402 treatment enhanced the cellular resistance to H_2O_2 cytotoxicity via the upregulation of the HO-1 and NQO1 proteins in both DP31 and DP296, regardless of FGF2 priming (Fig. 6).

Conversely, neither FGF2 priming nor RTA402 treatment affected the TAC of DPCs, and additive and/or synergistic effects were observed in both treatments (Fig. 4). Some previous studies indicated that FGF2 directly induces the expression of Nrf2[51–53], which may not be the case in DPCs. Because FGF2 priming did not

significantly affect Nrf2 and HO-1 expression (Supplemental Fig. 2) or promote the RTA402-induced expression of the HO-1 and NQO1 proteins (Fig. 6). Conversely, RTA402 treatment limitedly induced the expression of Nrf2 downstream genes. As shown in Supplemental Fig. 4, RTA402 did not affect the expression levels of catalase and GPx1/2, even though they are also RTA402/Nrf2 signaling downstream target genes[54,55]. Therefore, we hypothesized that the cell-specific epigenetic repressive regulatory mechanism of Nrf2 downstream genes[56,57] may be modified, and/or the cellular metabolism, including protein synthesis, may be facilitated by FGF2 priming. In fact, the osteoblast, odontoblast, and neuronal differentiation of DPCs are significantly promoted after FGF2 pre-treatment[58–61]. In any case, the combination of FGF2 priming with RTA402 treatment is considered to minimize donor effects and enhance antioxidant activity and cellular resistance to oxidative stress toxicity in DPCs.

What Is Desired for the Use of DPCs as a Cell Transplantation–Based Therapy for Acute-Phase SCI?

To exert their therapeutic efficacy, the transplanted DPCs should reach the action site, i.e., the injury epicenter. The transplanted cells should also overcome the high dose and concentration of ROS-induced cytotoxicity and secrete various cytokines and neurotrophic factors to modulate the immune response, prevent neuronal cell death, and promote axonal regeneration[16,17]. In fact, we have previously reported that the i.p. injection of a radical scavenger (edaravone) alone does not lead to locomotor recovery in the complete model, whereas the i.p. administration of edaravone enhances DPCs (DP31S), to promote locomotor-function recovery in combination with cell transplantation[23]. Here, because FGF2 not only enhanced the defense of DPC cells against oxidative stress via the RTA402 treatment but also promoted the migration of various MSCs[62,63], FGF2 priming was considered to enhance the capabilities of DPCs as cellular agents for SCI therapy. In fact, FGF2 priming tended to enhance the growth and migration (Fig. 1) of many DPC clones, with an increase in the expression levels of PAK1 and PAK2. PAKs are major regulators of cytoskeletal rearrangement and promote cell migration and invasion[64,65]. In addition, neither of the treatments attenuates the expression of major neurotrophic factors (Supplemental Fig. 6).

Therapeutic Effects of DPC Transplantation With Enhanced Antioxidant Capacity in SCI Mouse Models

Using the SCI mouse model, we demonstrated that DP296, which is a DPC clone originally without a therapeutic effect on SCI, promoted the regeneration of 5-HT⁺-nerve fiber, and improved BMS scores (Fig. 7) when the cells were

treated with both FGF2 and RTA402. Thus, beyond the clonal differences, both the RTA402 and FGF2 treatments may sufficiently enhance the resistance of DPCs to oxidative and nitrosative stress, which are widely accepted as secondary injury mechanisms in spinal cord tissue[16]. Furthermore, 5-HT$^+$-nerve fibers originating from the raphe nucleus play an important role in the generation of voluntary and coordinated motor functions[66,67]. In this study, transplantation of RTA402/FGF2-treated DPCs yielded an increase in 5-HT$^+$-nerve fibers below the caudal side of the lesion epicenter. Although the number of 5-HT$^+$-nerve fibers was small and the effect was insufficient to contribute to the recovery of coordinated movements, as assessed based on the BMS score, future optimizing studies in this direction could establish a curative strategy that generates the more pronounced effect of restoring motor function. For example, the modification of the route of administration and multiple dosing may be successful. In fact, various delivery methods for BMSC transplantation were investigated to effectively improve the locomotor function of SCI models, including intravenous, intraspinal, and intrathecal injections[65]; in contrast, some reports have indicated that intrathecal administration is significantly more effective than i.v. administration[68,69].

Conclusion

We have shown that the TAC and resistance to H_2O_2 cytotoxicity are important key factors underlying the DPC clonal differences in the effect of locomotor function recovery of SCI model animals after transplantation. For cell transplantation therapy in humans, not only the factors on the patient side, such as the degree of SCI, but also differences in the properties of the cells used for transplantation, which may affect functional recovery, should be considered. In this study, we demonstrated that RTA402 treatment combined with FGF2 priming may enhance the cytoprotective effects of DPCs against oxidative stress and reduce the clonal differences in therapeutic efficacy. As an alternative, allogeneic transplantation of HHH DPC clones, which have a high antioxidant activity and therapeutic efficacy and are less prone to immune rejection, may be an option. In fact, because the DP74 clone used in this study was derived from an HHH donor[70] and these cells have shown remarkable motor function recovery in a rat model of SCI (Fig. 1), establishing a DPC cell clone bank that is suitable for SCI treatment can be envisioned as a future regenerative medicine approach.

Author Contributions

All authors had full access to all the data in this study and take responsibility for the integrity of the data and the accuracy of the data analysis. H.S., S.F., and H.F. contributed to conceptualization. H.F., H.S., and K.T. contributed to methodology. H.F., H.S., K.N., K.N., M.Y., H.K., T.M., A.T., and T.T-K. contributed to investigation. H.S. contributed to formal analysis. H.F. and H.S. contributed to writing—original draft. H.F. contributed to writing—review and editing.

Availability of Data and Materials

All data required to evaluate the conclusions in the study are present in the paper and/or the Supplementary Materials. Additional data related to this paper may be available to researchers upon request.

Ethical Approval

This study was approved by the Ethics Committees of Gifu Pharmaceutical University and Gifu University and was performed following the Ethical Guidelines for Medical and Health Research involving Human Subjects in Japan and Ethical Guidelines for Human Genome/Gene Analysis Research in Japan (Gifu Pharmaceutical University approval numbers 23-1, 28-17, 29-44, 30-33, 1-1, 2-16, and 3-25; Gifu University approval numbers 19-144, 22-280, 24-375, 26-116, 26-422, 28-335, 29-323, and 5-10). All participants involved in the study provided written informed consent before study enrollment.

Statement of Human and Animal Rights

All experimental procedures involving animals were approved by the Animal Care and Research Committee of Gifu Pharmaceutical University (approval numbers 2014-289, 2015-172, 2019-010, 2019-036, 2020-056, 2021-056, and 2023-060) and were performed in compliance with the Guidelines for Management and Welfare of Experimental Animals of the US National Institutes of Health.

Statement of Informed Consent

Written informed consent was obtained from the patients for their anonymized information or legally authorized representatives for anonymized patient to be published in this article.

ORCID iD

Hidefumi Fukumitsu (iD) https://orcid.org/0000-0002-9279-9344

Supplemental Material

Supplemental material for this article is available online.

References

1. Shingu H, Ohama M, Ikata T, Katoh S, Akatsu T. A nation-wide epidemiological survey of spinal cord injuries in Japan from January 1990 to December 1992. Paraplegia. 1995;33(4):183–88.

2. Miyakoshi N, Suda K, Kudo D, Sakai H, Nakagawa Y, Mikami Y, Suzuki S, Tokioka T, Tokuhiro A, Takei H, Katoh S, et al. A nationwide survey on the incidence and characteristics of traumatic spinal cord injury in Japan in 2018. Spinal Cord. 2021;59(6):626–34.

3. GBD 2016 Traumatic Brain Injury and Spinal Cord Injury Collaborators. Global, regional, and national burden of traumatic brain injury and spinal cord injury, 1990-2016: a systematic analysis for the global burden of disease study 2016. Lancet Neurol. 2019;18(1):56–87.

4. Tsuji O, Sugai K, Yamaguchi R, Tashiro S, Nagoshi N, Kohyama J, Iida T, Ohkubo T, Itakura G, Isoda M, Shinozaki M, et al. Concise review: laying the groundwork for a first-in-human study of an induced pluripotent stem cell-based intervention for spinal cord injury. Stem Cells. 2019;37(1):6–13.

5. Kong H, Liu P, Li H, Zeng X, Xu P, Yao X, Liu S, Cheng CK, Xu J. Mesenchymal stem cell-derived extracellular vesicles: the novel therapeutic option for regenerative dentistry. Stem Cell Rev Rep. 2023;19(1):46–58.

6. Sharma A, Gupta S, Archana S, Verma RS. Emerging trends in mesenchymal stem cells applications for cardiac regenerative therapy: current status and advances. Stem Cell Rev Rep. 2022;18(5):1546–1602.

7. Tang QR, Xue H, Zhang Q, Guo Y, Xu H, Liu Y, Liu JM. Evaluation of the clinical efficacy of stem cell transplantation in the treatment of spinal cord injury: a systematic review and meta-analysis. Cell Transplant. 2021;30:9636897211067804.

8. Chai Y, Jiang X, Ito Y, Bringas P Jr, Han J, Rowitch DH, Soriano P, McMahon AP, Sucov HM, Han J, Rowitch DH, et al. Fate of the mammalian cranial neural crest during tooth and mandibular morphogenesis. Development. 2000;127(8):1671–79.

9. Dominici M, Le Blanc K, Mueller I, Slaper-Cortenbach I, Marini F, Krause D, Deans R, Keating A, Prockop DJ, Horwitz E. Minimal criteria for defining multipotent mesenchymal stromal cells. The international society for cellular therapy position statement. Cytotherapy. 2006;8(4):315–17.

10. Gronthos S, Brahim J, Li W, Fisher LW, Cherman N, Boyde A, DenBesten P, Robey PG, Shi S. Stem cell properties of human dental pulp stem cells. J Dent Res. 2002;81(8):531–35.

11. Collart-Dutilleul PY, Chaubron F, De Vos J, Cuisinier FJ. Allogenic banking of dental pulp stem cells for innovative therapeutics. World J Stem Cells. 2015;7(7):1010–21.

12. Ohkoshi S, Hirono H, Nakahara T, Ishikawa H. Dental pulp cell bank as a possible future source of individual hepatocytes. World J Hepatol. 2018;10(10):702–7.

13. Sakai K, Yamamoto A, Matsubara K, Nakamura S, Naruse M, Yamagata M, Sakamoto K, Tauchi R, Wakao N, Imagama S, Hibi H, et al. Human dental pulp-derived stem cells promote locomotor recovery after complete transection of the rat spinal cord by multiple neuro-regenerative mechanisms. J Clin Invest. 2012;122(1):80–90.

14. Song M, Lee JH, Bae J, Bu Y, Kim EC. Human Dental Pulp Stem Cells Are More Effective Than human bone marrow-derived mesenchymal stem cells in cerebral ischemic injury. Cell Transplant. 2017;26(6):1001–16.

15. Tran AP, Warren PM, Silver J. The biology of regeneration failure and success after spinal cord injury. Physiol Rev. 2018;98(2):881–917.

16. Bains M, Hall ED. Antioxidant therapies in traumatic brain and spinal cord injury. Biochim Biophys Acta. 2012;1822(5):675–84.

17. Kumamaru H, Kadoya K, Adler AF, Takashima Y, Graham L, Coppola G, Tuszynski MH. Generation and post-injury integration of human spinal cord neural stem cells. Nat Methods. 2018;15(9):723–31.

18. Nakano N, Nakai Y, Seo TB, Homma T, Yamada Y, Ohta M, Suzuki Y, Nakatani T, Fukushima M, Hayashibe M, Ide C. Effects of bone marrow stromal cell transplantation through CSF on the subacute and chronic spinal cord injury in rats. PLoS One. 2013;8(9):e73494.

19. Buzoianu-Anguiano V, Rivera-Osorio J, Orozco-Suárez S, Vega-García A, García-Vences E, Sánchez-Torres S, Jiménez-Estrada I, Guizar-Sahagún G, Mondragon-Caso J, Fernández-Valverde F, Madrazo I, et al. Single vs. Combined therapeutic approaches in rats with chronic spinal cord injury. Front Neurol. 2020;11:136.

20. Luo L, He Y, Wang X, Key B, Lee BH, Li H, Ye Q. Potential roles of dental pulp stem cells in neural regeneration and repair. Stem Cells Int. 2018;2018:1731289.

21. Wang D, Wang Y, Tian W, Pan J. Advances of tooth-derived stem cells in neural diseases treatments and nerve tissue regeneration. Cell Prolif. 2019;52(3):e12572.

22. Hosmani J, Assiri K, Almubarak HM, Mannakandath ML, Al-Hakami A, Patil S, Babji D, Sarode S, Devaraj A, Chandramoorthy HC. Proteomic profiling of various human dental stem cells—a systematic review. World J Stem Cells. 2020;12(10):1214–36.

23. Nagashima K, Miwa T, Soumiya H, Ushiro D, Takeda-Kawaguchi T, Tamaoki N, Ishiguro S, Sato Y, Miyamoto K, Ohno T, Osawa M, et al. Priming with FGF2 stimulates human dental pulp cells to promote axonal regeneration and locomotor function recovery after spinal cord injury. Sci Rep. 2017;7(1):13500.

24. Sugiyama K, Nagashima K, Miwa T, Shimizu Y, Kawaguchi T, Iida K, Tamaoki N, Hatakeyama D, Aoki H, Abe C, Morita H, et al. FGF2-responsive genes in human dental pulp cells assessed using a rat spinal cord injury model. J Bone Miner Metab. 2019;37(3):467–74.

25. Krifka S, Spagnuolo G, Schmalz G, Schweikl H. A review of adaptive mechanisms in cell responses towards oxidative stress caused by dental resin monomers. Biomaterials. 2013;34(19):4555–63.

26. Lee DS, Li B, Kim KS, Jeong GS, Kim EC, Kim YC. Butein protects human dental pulp cells from hydrogen peroxide-induced oxidative toxicity via Nrf2 pathway-dependent heme oxygenase-1 expressions. Toxicol In Vitro. 2013;27(2):874–81.

27. Kim NY, Ahn SG, Kim SA. Cinnamaldehyde protects human dental pulp cells against oxidative stress through the Nrf2/HO-1-dependent antioxidant response. Eur J Pharmacol. 2017;815:73–79.

28. Jiao Y, Niu T, Liu H, Tay FR, Chen JH. Protection against HEMA-induced mitochondrial injury in vitro by Nrf2 Activation. Oxid Med Cell Longev. 2019;2019:3501059.

29. Yagishita Y, Gatbonton-Schwager TN, McCallum ML, Kensler TW. Current landscape of NRF2 biomarkers in clinical trials. Antioxidants. 2020;9(8):716.

30. Sakashita M, Tanaka T, Inagi R. Metabolic changes and oxidative stress in diabetic kidney disease. Antioxidants. 2021;10(7):1143.

31. Takeda T, Tezuka Y, Horiuchi M, Hosono K, Iida K, Hatakeyama D, Miyaki S, Kunisada T, Shibata T, Tezuka K. Characterization of dental pulp stem cells of human tooth germs. J Dent Res. 2008;87(7):676–81.

32. Takeda-Kawaguchi T, Sugiyama K, Chikusa S, Iida K, Aoki H, Tamaoki N, Hatakeyama D, Kunisada T, Shibata T, Fusaki N, Tezuka K. Derivation of iPSCs after culture of human dental pulp cells under defined conditions. PLoS One. 2014;9(12):e115392.

33. Boulland JL, Lambert FM, Züchner M, Ström S, Glover JC. A neonatal mouse spinal cord injury model for assessing post-injury adaptive plasticity and human stem cell integration. PLoS One. 2013;8(8):e71701.

34. Basso DM, Beattie MS, Bresnahan JC. A sensitive and reliable locomotor rating scale for open field testing in rats. J Neurotrauma. 1995;12(1):1–21.

35. Basso DM, Fisher LC, Anderson AJ, Jakeman LB, McTigue DM, Popovich PG. Basso Mouse Scale for locomotion detects differences in recovery after spinal cord injury in five common mouse strains. J Neurotrauma. 2006;23(5):635–59.

36. Borges PA, Cristante AF, Barros-Filho TEP, Natalino RJM, Santos GBD, Marcon RM. Standardization of a spinal cord lesion model and neurologic evaluation using mice. Clinics. 2018;73:e293.

37. Hattori N, Nomoto H, Fukumitsu H, Mishima S, Furukawa S. Royal jelly and its unique fatty acid, 10-hydroxy-trans-2-decenoic acid, promote neurogenesis by neural stem/progenitor cells in vitro. Biomed Res. 2007;28(5):261–66.

38. Fukumitsu H, Soumiya H, Furukawa S. Knockdown of pre-mRNA cleavage factor Im 25 kDa promotes neurite outgrowth. Biochem Biophys Res Commun. 2012;425(4):848–53.

39. Whale A, Hashim FN, Fram S, Jones GE, Wells CM. Signaling to cancer cell invasion through PAK family kinases. Front Biosci. 2011;16(3):849–64.

40. Senapedis W, Crochiere M, Baloglu E, Landesman Y. Therapeutic potential of targeting PAK signaling. Anticancer Agents Med Chem. 2016;16(1):75–88.

41. Stetler-Stevenson WG, Gavil NV. Normalization of the tumor microenvironment: evidence for tissue inhibitor of metalloproteinase-2 as a cancer therapeutic. Connect Tissue Res. 2014;55(1):13–19.

42. Yamane K, Misawa H, Takigawa T, Ito Y, Ozaki T, Matsukawa A. Multipotent neurotrophic effects of hepatocyte growth factor in spinal cord injury. Int J Mol Sci. 2019;20(23):6078.

43. Díaz-Galindo MDC, Calderón-Vallejo D, Olvera-Sandoval C, Quintanar JL. Therapeutic approaches of trophic factors in animal models and in patients with spinal cord injury. Growth Factors. 2020;38(1):1–15.

44. Muheremu A, Shu L, Liang J, Aili A, Jiang K. Sustained delivery of neurotrophic factors to treat spinal cord injury. Transl Neurosci. 2021;12(1):494–511.

45. Bressan E, Ferroni L, Gardin C, Pinton P, Stellini E, Botticelli D, Sivolella S, Zavan B. Donor age-related biological properties of human dental pulp stem cells change in nanostructured scaffolds. PLoS One. 2012;7(11):e49146.

46. Kellner M, Steindorff MM, Strempel JF, Winkel A, Kühnel MP, Stiesch M. Differences of isolated dental stem cells dependent on donor age and consequences for autologous tooth replacement. Arch Oral Biol. 2014;59(6):559–67.

47. Vakhrushev IV, Vdovin AS, Strukova LA, Yarygin KN. Variability of the phenotype and proliferation and migration characteristics of human mesenchymal stromal cells derived from the deciduous teeth pulp of different donors. Bull Exp Biol Med. 2016;160(4):525–29.

48. Lee S, Lee EK, Kang DH, Lee J, Hong SH, Jeong W, Kang SW. Glutathione peroxidase-1 regulates ASK1-dependent apoptosis via interaction with TRAF2 in RIPK3-negative cancer cells. Exp Mol Med. 2021;53(6):1080–91.

49. Itoh K, Mimura J, Yamamoto M. Discovery of the negative regulator of Nrf2, Keap1: a historical overview. Antioxid Redox Signal. 2010;13(11):1665–78.

50. Zhuang C, Miao Z, Sheng C, Zhang W. Updated research and applications of small molecule inhibitors of Keap1-Nrf2 protein-protein interaction: a review. Curr Med Chem. 2014;21(16):1861–70.

51. Tong G, Liang Y, Xue M, Chen X, Wang J, An N, Wang N, Chen Y, Wang Y, Jin L, Cong W. The protective role of bFGF in myocardial infarction and hypoxia cardiomyocytes by reducing oxidative stress via Nrf2. Biochem Biophys Res Commun. 2020;527(1):15–21.

52. Chen X, Tong G, Chen S. Basic fibroblast growth factor protects against liver ischemia-reperfusion injury via the Nrf2/Hippo signaling pathway. Tissue Cell. 2022;79:101921.

53. Wang L, Cheng F, Pan R, Cui Z, She J, Zhang Y, Yang X. FGF2 rescued cisplatin-injured granulosa cells through the NRF2-autophagy pathway. Int J Mol Sci. 2023;24(18):14215.

54. Tian C, Gao L, Zhang A, Hackfort BT, Zucker IH. Therapeutic effects of Nrf2 activation by bardoxolone methyl in chronic heart failure. J Pharmacol Exp Ther. 2019;371(3):642–51.

55. Kurosaki Y, Imoto A, Kawakami F, Ouchi M, Morita A, Yokoba M, Takenaka T, Ichikawa T, Katagiri M, Nielsen R, Ishii N. In vitro study on effect of bardoxolone methyl on cisplatin-induced cellular senescence in human proximal tubular cells. Mol Cell Biochem. 2022;477(3):689–99.

56. Zhang J, Pan W, Zhang Y, Tan M, Yin Y, Li Y, Zhang L, Han L, Bai J, Jiang T, Li H. Comprehensive overview of Nrf2-related epigenetic regulations involved in ischemia-reperfusion injury. Theranostics. 2022;12(15):6626–45.

57. McCord JM, Gao B, Hybertson BM. The complex genetic and epigenetic regulation of the Nrf2 pathways: a review. Antioxidants. 2023;12(2):366.

58. He H, Yu J, Liu Y, Lu S, Liu H, Shi J, Jin Y. Effects of FGF2 and TGFbeta1 on the differentiation of human dental pulp stem cells in vitro. Cell Biol Int. 2008;32(7):827–34.

59. Osathanon T, Nowwarote N, Pavasant P. Basic fibroblast growth factor inhibits mineralization but induces neuronal differentiation by human dental pulp stem cells through a FGFR and PLCgamma signaling pathway. J Cell Biochem. 2011;112(7):1807–16.

60. Qian J, Jiayuan W, Wenkai J, Peina W, Ansheng Z, Shukai S, Shafei Z, Jun L, Longxing N. Basic fibroblastic growth factor

affects the osteogenic differentiation of dental pulp stem cells in a treatment-dependent manner. Int Endod J. 2015;48(7):690–700.

61. Shimabukuro Y, Ueda M, Ozasa M, Anzai J, Takedachi M, Yanagita M, Ito M, Hashikawa T, Yamada S, Murakami S. Fibroblast growth factor-2 regulates the cell function of human dental pulp cells. J Endod. 2009;35(11):1529–35.

62. Peng L, Ye L, Zhou XD. Mesenchymal stem cells and tooth engineering. Int J Oral Sci. 2009;1(1):6–12.

63. Gagliardi PA, di Blasio L, Primo L. PDK1: a signaling hub for cell migration and tumor invasion. Biochim Biophys Acta. 2015;1856(2):178–88.

64. Chen L, Bi S, Hou J, Zhao Z, Wang C, Xie S. Targeting p21-activated kinase 1 inhibits growth and metastasis via Raf1/MEK1/ERK signaling in esophageal squamous cell carcinoma cells. Cell Commun Signal. 2019;17(1):31.

65. Sławińska U, Miazga K, Jordan LM. The role of serotonin in the control of locomotor movements and strategies for restoring locomotion after spinal cord injury. Acta Neurobiol Exp. 2014;74(2):172–87.

66. Ghosh M, Pearse DD. The role of the serotonergic system in locomotor recovery after spinal cord injury. Front Neural Circuits. 2014;8:151.

67. Oliveri RS, Bello S, Biering-Sørensen F. Mesenchymal stem cells improve locomotor recovery in traumatic spinal cord injury: systematic review with meta-analyses of rat models. Neurobiol Dis. 2014;62:338–53.

68. Paul C, Samdani AF, Betz RR, Fischer I, Neuhuber B. Grafting of human bone marrow stromal cells into spinal cord injury: a comparison of delivery methods. Spine. 2009;34(4):328–34.

69. Liu G, Zhao Z, Wang H, Hao C, Wang W, Zhang C, Wang T, Li X, Xi J, Li S, Long H, et al. Therapeutic efficacy of human mesenchymal stem cells with different delivery route and dosages in rat models of spinal cord injury. Cell Transplant. 2022;31:9636897221139734.

70. Shimizu Y, Takeda-Kawaguchi T, Kuroda I, Hotta Y, Kawasaki H, Hariyama T, Shibata T, Akao Y, Kunisada T, Tatsumi J, Tezuka KI. Exosomes from dental pulp cells attenuate bone loss in mouse experimental periodontitis. J Periodontal Res. 2022;57(1):162–72.